

Received December 10, 2018, accepted December 28, 2018, date of current version January 29, 2019.

Digital Object Identifier 10.1109/ACCESS.2019.2891699

# Uncertainty-Aware Computational Tools for Power Distribution Networks Including Electrical Vehicle Charging and Load Profiles

GIAMBATTISTA GRUOSSO<sup>1</sup>, (Senior Member, IEEE),  
GIANCARLO STORTI GAJANI<sup>1</sup>, (Senior Member, IEEE),  
ZHENG ZHANG<sup>2</sup>, (Member, IEEE),  
LUCA DANIEL<sup>3</sup>, (Senior Member, IEEE),  
AND PAOLO MAFFEZZONI<sup>1</sup>, (Senior Member, IEEE)

<sup>1</sup>Politecnico di Milano, Deib, 20133 Milan, Italy

<sup>2</sup>Department of Electrical and Computer Engineering, University of California at Santa Barbara, Santa Barbara, CA 93106, USA

<sup>3</sup>Massachusetts Institute of Technology, Cambridge, MA 02139, USA

Corresponding author: Giambattista Gruosso (giambattista.gruosso@polimi.it)

**ABSTRACT** As new services and business models are being associated with the power distribution network, it becomes of great importance to include load uncertainty in predictive computational tools. In this paper, an efficient uncertainty-aware load flow analysis is described which relies on generalized polynomial chaos and stochastic testing methods. It is described how the method can be implemented in order to account for real data-based load profiles due to two different usage models: residential loads and electrical vehicle charging profiles. Hence, it is shown how some relevant information affecting the quality of service can be deduced by means of non-elementary post-processing computations. The proposed technique is tested by using a benchmark scenario for typical European low voltage networks, considering the variation of both residential loads and EV charging profiles. The results are compared with the same simulation done by means of the Monte Carlo methodology. The consideration done during the analysis will be useful to clarify the application of the methodology but also to understand the effect of load variations on the grid characteristic quantities.

**INDEX TERMS** Distribution network, load uncertainty, variability analysis, load forecasting, EV charging profiles, electrical vehicles.

## I. INTRODUCTION

Electrical distribution networks are a specific kind of large scale systems that are designed to provide the required power to the loads while ensuring stability of node voltages, i.e. the quality of service. The recent trends towards the exploitation of renewable energy sources and the integration of new services, e.g. the charging of electrical vehicles, are introducing a remarkable variability of the powers that are delivered and/or absorbed at the terminal loads. Such a variability can jeopardize the stability of the network and the quality of service [1]. For such reasons, it is now noticeable the key role that uncertainty-aware computational tools can play during the design and real time control of power

distribution circuits [2]–[5]. In fact, such tools can provide a comprehensive view of the overall network: they can predict bus voltages and line currents variations at network points that can hardly be measured.

The mainstream network uncertainty analysis approach adopts probabilistic models for the loads and uses repeatedly deterministic Load Flow (LF) analysis within a Monte Carlo (MC) iterative procedure. This approach, which is commonly referred to as Probabilistic Load Flow (PLF) analysis, can however be very time consuming and thus unpractical. Indeed, many open issues remain in PLF analysis. A first relevant issue is connected to modeling load uncertainty in a realistic way. Load modeling is commonly

based on statistical analyses of available customer profile data that are collected and analyzed for several network areas and utility types (e.g. residential, commercial and industrial, electrical vehicles). Several modeling approaches exist, some of these are built on the aggregated data about the total load of the network, some others on the analysis of the statistical distribution of the loads at each node. In order to account for the interplay of many independent uncertain loads (i.e. variations in the active powers supplied at the different phases of the network) a great number of MC runs is needed to achieve a satisfactory statistical description. In fact, even though loads uncertainty can commonly be assumed to be Gaussian distributed, the nonlinear nature of load flow leads to state variable variations, e.g. maximum voltage at nodes or lines current, that are non-Gaussian-distributed. In this case, the statistical information about mean value and variance of an electric variable is not enough to describe it properly and the detailed Probability Density Function (PDF) shape is required for further inferences. The accurate determination of PDF with MC method can require tens of thousands repeated load flow analyses thus becoming very time consuming.

To address the above issues, in this paper we focus on an efficient uncertainty quantification method recently presented in the literature [6], [7], and describe its specific application to the PLF problem [8], [9]. The method is based on generalized Polynomial Chaos (gPC) expansion and Stochastic Testing (ST) algorithm and is denoted as gPC+ST. Compared to other approximate techniques adopted for PLF analysis [2], [3], the gPC+ST method exhibits some features that make it well suitable for PLF applications. In fact, gPC+ST can be applied in connection to any available deterministic load flow solver without having to modify the codes. Furthermore, the gPC+ST method can deal with truly nonlinear problems that provide non-Gaussian-distributed output variables even in the case of uncertainty sources being modelled as Gaussian-distributed parameters. This is indeed the case for load flow analysis formulated in terms of node voltages and powers.

As a first original contribution of this paper, we describe how the gPC+ST method can be implemented while accounting for real data-based load profiles. We will focus on two different types of load. The first is a mix of residential and commercial loads, while the second represents the power used to recharge electric vehicles. The two load categories are different one another, however, they are well suited to be interpreted in a unified probabilistic way.

The profiles of the residential and commercial loads are considered from the low voltage side and the data are provided by the benchmark IEEE European low voltage test feeder network [10]. The benchmark is also used as a test network to demonstrate the validity of our method. The data relating to the recharging of electric vehicles, on the other hand, are measured and acquired in the context of the Italian project Teinvein [11] and represent a special case of recharging: low voltage and on recharging stations consisting

of several parallel recharging points. These are used by a very specific fleet of vehicles that are the object of the cited project.

A second contribution of our research is showing how the proposed method can be exploited to predict the detailed probability distribution and variability interval of a set of Quantities of Interest (QoI) that directly impact on the quality of service. Such variables can include the peak and minimum values assumed by the three phase voltages at some observable nodes as well as more general quantities that require non-elementary post-processing computations. In fact, real load profiles tend to produce sharp fluctuations in time of the node voltages. However, only the peak voltages that last for a sufficiently long period of time actually affect the quality of service. In this paper, we show how, for a given degree of variability of the load profiles, the proposed gPC+ST method can be exploited to deduce the probability that a node voltage will exceed a safe limit for a time duration  $W$ .

The remainder of the paper is organized as follows: Sec. II reviews the deterministic load flow analysis; in Sec. III, we model load uncertainty and present the idea behind the gPC+ST method while in Sec. IV we provide the computational details. In Sec. V, we describe a relevant example of non-elementary post-processing computation and, finally, in Sec. VI we illustrate some application results in different scenarios.

## II. LOAD FLOW ANALYSIS

An electrical distribution system can be seen as a set of buses connected to each other by lines. Devices and equipment capable of providing or absorbing active and reactive power are connected to each one of the buses. The load flow problem consists in finding the set of voltages, i.e. the magnitude and angle, which, together with the network impedances, produces the load flows that are known to be correct at the system terminals. Assuming that the network is made of  $N$  buses and  $N_l$  lines, the problem is formulated mathematically as a set of nonlinear equations [12], [13] of the type:

$$\mathbf{F}_n(\vec{\mathbf{V}}) = \mathbf{S}_n - \mathbf{V}_n \sum_{i=1}^N \mathbf{Y}_{ni} \mathbf{V}_i^* = \mathbf{0} \quad (1)$$

for  $n = 1, \dots, N$ . In (1),  $\mathbf{S}_n = P_n + jQ_n$  denotes the complex power at node  $n$  where  $P_n$  and  $Q_n$  are the active and reactive powers respectively,  $\mathbf{V}_n$  is the node voltage phasor, while  $\mathbf{Y}_{ni}$  are the entries of the bus admittance matrix. Node voltage phasors are collected into vector  $\vec{\mathbf{V}}$ .

Network terminations are specified by imposing the known active and reactive powers  $P_n$ ,  $Q_n$  absorbed or delivered by loads. Load conditions vary in time and thus the associated powers become functions of time,  $P_n(t)$ ,  $Q_n(t)$ . Let us consider a given observation time period (e.g. a day or a week), that is discretized into a sequence of  $N_t$  equally-spaced time instants  $t_m = m \cdot \Delta t$ , over which the load profiles are given. Node voltage waveforms  $\mathbf{V}_n(t)$  are calculated by repeatedly solving the nonlinear problem (1) over the sequence of

time instants  $t_m$ . In doing that, the network state computed at time  $t_m$  is used as the solver initial condition at next time  $t_{m+1}$ .

### III. UNCERTAINTY QUANTIFICATION WITH GENERALIZED POLYNOMIAL CHAOS

#### A. MODELING LOAD VARIABILITY

In the literature, load modeling is commonly achieved by exploiting historic data sets that are collected and analyzed for several network areas and utility types (e.g residential, commercial and industrial, electrical vehicles). Coherently with such an approach, the gPC-based methodology that we illustrate in this paper allows accounting for the typical time evolution (i.e. the chronological variation) of the most common power load profiles. The first type of loads herein considered are residential and commercial ones: these are single-phase loads connected at different nodes of the network. To realistically reproduce the effects that these loads could have on the network, we consider 55 different power profiles  $p_n^{RC}(t)$ , with  $n = 1, \dots, 55$ , selected among the ones provided with the benchmark test case [10]. These data represent with good approximation what can happen in a daily scenario. The 55 profiles are randomly subdivided into three roughly equivalent sets, and each set is then connected to one of the three phase lines (each load is connected to a different node). Fig. 1 shows the average value (i.e., the ensemble average) and the variability range of the loads for each phase line. It is evident how residential and commercial power demand is higher over certain time slots of the day where it can exhibit significant variability. In order to reproduce the uncertainty of the total power demand at each phase line the active power at the  $n$ th node is written as:

$$P_n(t) = p_n^{RC}(t) \left[ 1 + \sigma_n^{RC} \xi_j \right] \quad (2)$$

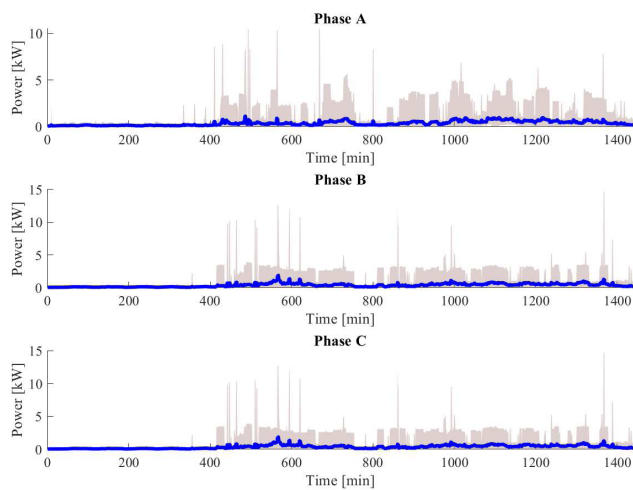


**FIGURE 1.** Load variability in the three phases for the residential and commercial loads. The blue line present the mean value and the shadowed region the variability range.

where we remind that  $p_n^{RC}(t)$  is the (known) nominal power profile over the time period. In (2),  $\xi_j$  denotes a zero-mean Gaussian-distributed statistical variable having unitary variance, i.e.  $\langle \xi_j \rangle = 0$  and  $\langle \xi_j^2 \rangle = 1$ , while  $\sigma_n^{RC}$  is a scaling constant that determines the degree of variability.

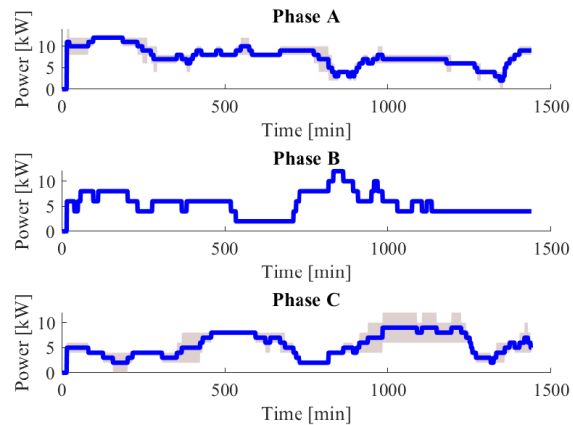


**FIGURE 2.** Load variability in the three phases for the Electrical Vehicle Charging Stations. The blue line present the mean value and the shadowed region the variability range.

The second type of loads that we consider in this paper is the active power absorbed by EV charging stations. Fig. 2 shows some typical time evolutions of the EV power profiles  $p^{EV}(t)$  measured during the research activity of the Italian Project TEINVEIN [11]. The electric vehicles that are considered in this project compose the fleet of a very successful urban car sharing service. These vehicles are recharged by service personnel at times of day with a distribution that is essentially optimized for the car sharing purposes: i.e. having the maximum number of charged vehicles at peak usage times.

Similarly to what has been done for commercial and residential profiles, the EV profiles are randomly grouped into three sets and connected to the three phase lines. To the aim of reproducing the effect of EV loads and their statistical uncertainty, a second active power contribution

$$P'_n(t) = p^{EV}(t) \left[ 1 + \sigma_n^{EV} \xi_j \right] \quad (3)$$

is added at the  $n$ th node, where  $\sigma_n^{EV}$  is the degree of variability for the EV profile. Compared to the first type of loads, EV profiles exhibit some different features: they are more continuous with time and involve higher power consumptions. The addition of EV profiles thus enriches the scenario of the probabilistic analysis. We finally remark that the number of statistical parameters  $\xi_j$  employed does not necessarily corresponds to the number of nodes or loads, in fact sets of power profiles at different nodes can be scaled by the same statistical parameter. As an instance, in Sec. VI, devoted to applications, we will consider only three statistical  $\xi_j$  variables, one for each phase line.

**B. GENERALIZED POLYNOMIAL CHAOS**

We consider a probabilistic problem where the uncertainty in the load power profiles is described by means of  $l$  stochastic parameters  $\xi_r$  modeling active power variability as in (2). Stochastic parameters are collected in the vector  $\vec{\xi} = [\xi_1, \xi_2, \dots, \xi_l]$ . The gPC method consists in adopting generalized polynomial chaos expansions for the node voltages. Depending on the numerical technique used to solve the gPC problem, the variables that have to be expanded can be all of the node voltages in the network or a subset of them, obviously these voltages are in general represented as complex phasors including magnitude and phase information. In some cases, the variables that we need to expand are limited to the quantities that we want to monitor: they may be the magnitude of some node voltages or line currents at a given time or the peak or minimum value assumed over a time period. In what follows, we will generically denote as  $V(t, \vec{\xi})$  one of these variables. Under the mild hypothesis that  $V(t, \vec{\xi})$  has finite variance (i.e. it is a second-order stochastic process), it can be approximated by an order- $\beta$  truncated series [14]

$$V(t, \vec{\xi}) \approx \sum_{i=1}^{N_b} c_i(t) H_i(\vec{\xi}), \tag{4}$$

formed by  $N_b$  multi-variate basis functions  $H_i(\vec{\xi})$  weighted by unknown polynomial chaos coefficients  $c_i(t)$ . The main feature in expression (4) is that the dependence of  $V(\cdot)$  on the deterministic variable time, which is incorporated into coefficients  $c_i(t)$ , is separated by its dependence on statistical parameters  $\vec{\xi}$  represented by basis functions  $H_i(\vec{\xi})$ .

Each multi-variate basis function is given by the product

$$H_i(\vec{\xi}) = \prod_{r=1}^l \phi_{i_r}(\xi_r) \tag{5}$$

where  $\phi_{i_r}(\xi_r)$  is a univariate orthogonal polynomial of degree  $i_r$  whose form depends on the density function of the  $r$ th parameter  $\xi_r$ . For instance,  $\phi_{i_r}(\xi_r)$  are Hermite polynomials if  $\xi_r$  is a Gaussian-distributed variable, while  $\phi_{i_r}(\xi_r)$  are Legendre polynomials if  $\xi_r$  is a uniformly distributed variable. A complete list of correspondence between several typical stochastic distributions and associated orthogonal polynomials can be found in [14].

For a given number of parameters  $l$  and series expansion truncation order  $\beta$ , the degrees  $i_r$  of univariate polynomials in (5) forming  $H_i(\vec{\xi})$ , for  $r = 1, \dots, l$ , satisfy the following relation

$$\sum_{r=1}^l i_r \leq \beta. \tag{6}$$

For generic truncation order  $\beta$  and number of parameters  $l$ , the number of gPC basis functions is given by [6]

$$N_b = \frac{(\beta + l)!}{\beta! l!}. \tag{7}$$

**IV. COMPUTING THE GPC COEFFICIENTS**

There are two different mainstream approaches for computing the gPC expansion coefficients in (4): Galerkin Projection and Collocation Method [15].

**A. GALERKIN PROJECTION (GP)**

Galerkin projection is an *intrusive* numerical technique that requires modifying the LF code (1). In accordance with this method, a gPC expansion of the type (4) is adopted for each unknown nodal voltage  $\mathbf{V}_n(t)$ , i.e.

$$\mathbf{V}_n(t, \vec{\xi}) \approx \sum_{i=1}^{N_b} \mathbf{c}_i^n(t) H_i(\vec{\xi}), \tag{8}$$

leading to  $N_b \times N$  unknown  $\mathbf{c}_i^n$  coefficients that are complex variables. Such coefficients are determined by plugging the expansions (8) into (1) and then projecting the resulting nodal equations along the  $N_b$  basis functions. This results in a very large nonlinear system of size  $N_b \times N$ , i.e.

$$(\mathbf{F}_n(\vec{\mathbf{V}}(\vec{\xi}), H_i(\vec{\xi}))_{\Omega} = \mathbf{0}, \tag{9}$$

for  $n = 1, \dots, N$  and  $i = 1, \dots, N_b$ , where  $\langle \cdot \rangle_{\Omega}$  denotes the inner product in the stochastic space [6]. The solution of (9) requires a significant computational effort both in terms of time and allocated memory. As an example, consider the case of a distribution network with  $N = 100$  nodes, and suppose to perform stochastic Galerkin with  $l = 3$  statistical parameters and expansion order  $\beta = 3$ . In this case,  $N_b = 20$ , so that the nonlinear system to be solved has size  $N_b \times N = 2,000$ . Due to problem nonlinearity, equations (9) tend to be strongly coupled among them (i.e. intermodulation of expansion coefficients) so that the computational time required for solving the system tends to grow as a power of two of the system size, i.e. about  $(N_b \times N)^2$ . In our example, the computational time for solving the Galerkin problem is about  $400 \times$  longer than that needed for a single LF analysis. The GP computational time grows very rapidly with the number of statistical parameters thus limiting the applicability of the method to networks of small size.

**B. STOCHASTIC COLLOCATION (SC)**

SC is a *nonintrusive* method that can be combined with any LF formulation (1) without modifying the implementation codes. A second advantage of the SC method is that gPC expansion (4) is adopted limitedly to the set of network variables that we want to evaluate, i.e. the peak value of some monitoring node voltages. In what follows, we will focus on a recently proposed efficient implementation of SC method referred to as Stochastic Testing (ST) method. In accordance with the collocation-based Stochastic Testing (ST) [6], the  $N_b$  unknown coefficients  $c_j(t)$  in the series (4) are calculated by properly selecting  $N_s = N_b$  testing points  $\vec{\xi}^k$ , for  $k = 1, \dots, N_s$  in the stochastic space where  $V_k(t) = V(t, \vec{\xi}^k)$  is calculated with a deterministic LF analysis.

At each testing point, the series expansion (4) is enforced to fit *exactly* (i.e., the polynomials interpolate the samples) the values  $V_k(t)$ .

Mathematically, this results in the following linear system

$$\mathbf{M}\vec{c}(t) = \vec{V}(t), \quad (10)$$

where  $\vec{c}(t) = [c_1(t), \dots, c_{N_b}(t)]^T$  and  $\vec{V}(t) = [V_1(t), \dots, V_{N_s}(t)]^T$  are the column vectors collecting the unknown coefficients and node voltage values respectively.

The  $N_b \times N_b$  square matrix  $\mathbf{M} = \{a_{k,i}\} = \{H_i(\vec{\xi}^k)\}$  collects the gPC basis functions evaluated at the testing points, i.e.

$$\mathbf{M} = \begin{bmatrix} H_1(\vec{\xi}^1) & \dots & H_{N_b}(\vec{\xi}^1) \\ \vdots & \ddots & \vdots \\ H_1(\vec{\xi}^{N_s}) & \dots & H_{N_b}(\vec{\xi}^{N_s}) \end{bmatrix}. \quad (11)$$

It is worth noting that matrix  $\mathbf{M}$  only depends on the selected basis functions and testing points, so that it can be precalculated, inverted and used for any  $t = t_m$  as follows:

$$\vec{c}(t_m) = \mathbf{M}^{-1} \vec{V}(t_m). \quad (12)$$

The ST method enables handling PLF problems with larger size and larger number of parameters.

The selection of the testing points  $\vec{\xi}^k$  in the stochastic space is done so to ensure the highest numerical accuracy of the gPC-based interpolation scheme and of the associated statistical description. This is achieved by considering as testing points the  $(\beta + 1)^l$  Gauss quadrature nodes in the  $l$ -dimensional stochastic space. Since the number  $(\beta + 1)^l$  of nodes is greater than the number  $N_b$  of basis functions defined in (7), a subset formed by  $N_s = N_b$  quadrature nodes has to be selected as testing points in order to make problem (12) well posed. A possible method for selecting the subset of testing points among the quadrature nodes is presented in [6].

## V. NON-ELEMENTARY POST-PROCESSING COMPUTATION

Once the coefficients  $c_j(t)$  are computed, the mean value and standard deviation of an observable variable  $V(t, \vec{\xi})$  can easily be determined [6]. Furthermore, and even more importantly, the gPC expansion (4) provides a compact model for the  $V(t, \vec{\xi})$  multi-dimensional dependence. This enables repeated evaluations of  $V(t, \vec{\xi})$  for large numbers of uncertainty vector realizations  $\vec{\xi}^k$  in very short times (one million evaluations require only few seconds on a quad-core computer) and the determination of the detailed shape of the PDF. Such accurately-computed PDF can then be exploited in further inferences such as the evaluation of the variability interval of the observable variable (with a certain confidence degree).

More general information can further be deduced through non-elementary post-processing computations. In what follows, we illustrate two examples of non-elementary computing that are relevant for PLF applications.

### A. PEAK VOLTAGE LASTING FOR A TIME DURATION $W$

In this first example, we focus on the determination of the probability that a node voltage will exceed a safe limit  $V_L$  for a time duration  $W$ . To this aim, and using the notation introduced in Sec. II, we consider the generic time window of duration  $W = n_w \Delta t$  (with  $n_w \ll N_t$ ) corresponding to the time subgrid  $t_{m+1}, \dots, t_{m+n_w}$  and the related samples of the observable node voltage, i.e.

$$V(t_{m+1}, \vec{\xi}), \dots, V(t_{m+n_w}, \vec{\xi}). \quad (13)$$

We denote

$$\alpha_m(\vec{\xi}) = \min\{V(t_{m+1}, \vec{\xi}), \dots, V(t_{m+n_w}, \vec{\xi})\} \quad (14)$$

the minimum of such voltage values. It results that the value  $\alpha_m$  is exceeded (or equated) by the considered node voltage for all the duration  $W$ . As a consequence, the maximum value of  $\alpha_m$  calculated over all possible time windows of duration  $W$ , i.e.

$$V_W^{peak}(\vec{\xi}) = \max_{m \in (0, \dots, N_t - n_w)} \{\alpha_m(\vec{\xi})\} \quad (15)$$

provides the maximum voltage level that is exceeded (or equated) by the node voltage for a time period  $W$ . For a given degree of variability of the power load profiles, the PDF  $f_W(V)$  of the quantity of interest  $V_W^{peak}(\vec{\xi})$  can be computed by means of the proposed gPC+ST method and post-processing expressions (14) and (15). After that, the integral

$$\int_{V_L}^{\infty} f_W(V) dV \quad (16)$$

supplies the probability that the safe limit  $V_L$  is exceeded by the considered node voltage for a time duration  $W$ .

### B. VOLTAGE UNBALANCE FACTOR

Probabilistic fluctuations of node voltages can induce some unbalance among the line phases eventually affecting the quality of service in accordance with the IEC EN 50160. The percentage Voltage Unbalance Factor (VUF) is just a measure of such a quality deterioration. It is defined as the ratio of the negative voltage sequence component  $V_n$  to the positive voltage sequence component  $V_p$  [16], i.e.

$$\text{VFU} = \frac{|V_n|}{|V_p|} \cdot 100, \quad (17)$$

with

$$V_n = \frac{V_{AB} + a^2 \cdot V_{BC} + a \cdot V_{CA}}{3} \quad (18)$$

and

$$V_p = \frac{V_{AB} + a \cdot V_{BC} + a^2 \cdot V_{CA}}{3}, \quad (19)$$

where  $V_{AB}, V_{BC}, V_{CA}$  are the phasors of the unbalanced line voltages while  $a = \exp(j120^\circ)$  and  $a^2 = \exp(j240^\circ)$ . By means of the gPC+ST method and post-processing expression (17), the detailed PDF of the maximum VUF

over a given observable time window (e.g. a day) can be determined. Furthermore, combining (17) with (14) and (15), it is possible to deduce the PDF of the maximum VUF, i.e.  $VUF_W^{peak}$ , lasting for a sufficiently long time  $W$  (e.g. 15 minutes) and thus able to deteriorate the quality of service.

## VI. SIMULATION FRAMEWORK AND NUMERICAL RESULTS

A low-voltage distribution network, typical of Europe, was chosen to demonstrate the method. It is a Radial network, described through buses and lines with their impedance. The phenomena of voltage drop and coupling between the phases are therefore not negligible and it is precisely these effects that are analyzed in order to determine the quality of the network.

Such a test network, published by the Test Feeders Working Group of the Distribution System Analysis Subcommittee of the *Power Systems Analysis, Computing, and Economics Committee* (PSACE), provides a valid benchmark for researchers willing to study low voltage feeders which are common in Europe [10]. Fig. 3 shows the tree topology of the benchmark power distribution network that we will use as the case study: the markers represent the loads and the colors the load phase connection. In the figure the Charging Stations and the observation point are also shown.

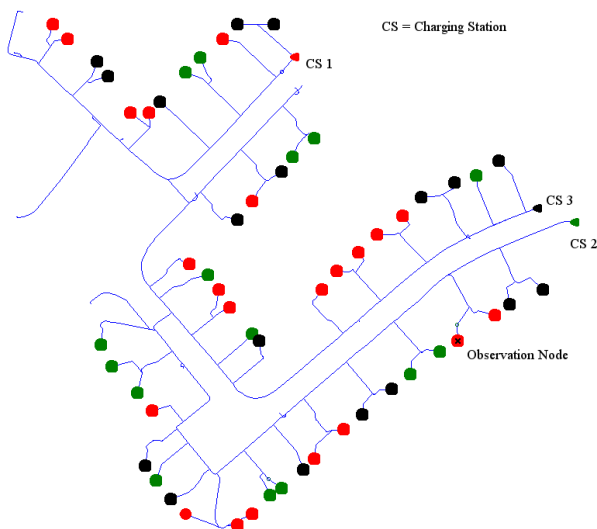


**FIGURE 3.** Topology of the IEEE low voltage European test feeder used in this research as a benchmark example: the loads are applied to the node with the circle marker (Red = phase A, Black = phase B, Green = phase C). The charging stations CS for each phase are shown.

In our implementation, the gPC+ST code developed at *Massachusetts Institute of Technology* [6] and written in Matlab is interfaced with the Load Flow deterministic solver OpenDSS [17]. Such a simulation framework is used to perform variability analysis of the test IEEE European low voltage test feeder shown in Fig. 3. The LV test feeder model is composed of 906 low voltage nodes, connected by

905 branches. The network is radial, with 55 load buses. In this work, we assume that all of the powers at the termination are given as 1-phase loads. Such loads are assigned to 55 nodes and their shapes are provided by the benchmark, as 1 minute time series, over 24h time span [10]. In the following, we consider three different scenarios. The first is where only residential/commercial loads are present. In the second two scenarios we consider also the presence of Electrical Vehicles. In one case by keeping the residential loads fixed and varying only the contribution of electric vehicles, in the other by varying both types of load but with different values of  $\sigma$ .

### A. SCENARIO I: VARIATION OF LOAD WITHOUT EV

In what follows, we describe one possible application of the proposed variability analysis where we consider statistical variations of the *total power* of the loads assigned to a line phase. To this aim, and in accordance with the load model (2), we assume that the active powers  $P_n(t)$  of all of the nodes assigned to a given phase line, e.g. Phase A, are scaled by the same  $\xi$  Gaussian statistical parameter, e.g.  $\xi_1$ . As a result, three statistically independent parameters  $\xi_1$ ,  $\xi_2$  and  $\xi_3$  are taken into account for the three phase lines A, B, C, respectively. The degrees of variability are constant and set to  $\sigma_{p1} = \sigma_{p2} = \sigma_{p3} = 0.2$  for all of the loads connected to the three phase lines. This choice is completely arbitrary and was made to ensure that the scaling factor, comprised between 0 and 1, induces a variation no greater than 20 %.

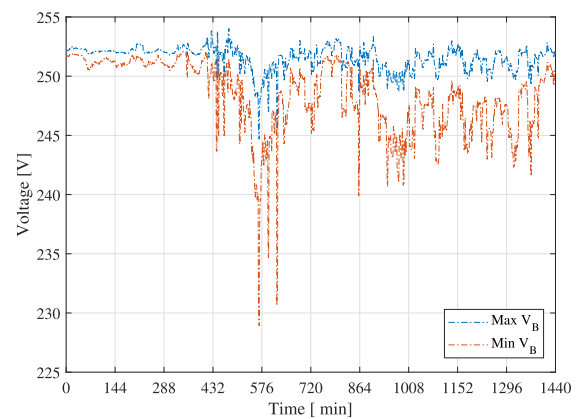


**FIGURE 4.** Time domain curves of the envelope of maxima and minima in the 20 sampling points.

Assuming a  $\beta = 3$  expansion order, 20 testing points are generated in the statistical space and for each one of them a deterministic load flow analysis is performed. Fig. 4 reports the envelope of the voltage waveforms of the phase B minima and maxima at node 898 evaluated in the 20 sample points (i.e. a given set of parameters  $\vec{\xi}$ ), simulated with OpenDSS, while in Fig. 5 the boxplot of the phase B voltage is reported for each gPC sample. Voltage waveforms exhibit sharp fluctuations over the day due to the time varying nature of the load profiles. In addition, the daily peak and minimum of the phase voltages undergo statistical variations due to the

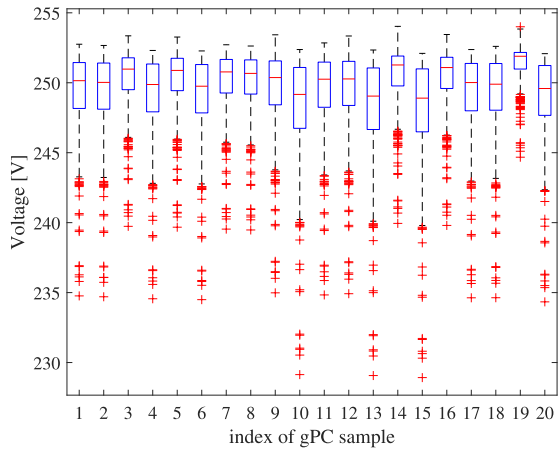


**FIGURE 5.** Scenario I. For each gPC sample the variation of the phase B voltage waveform is plotted. The red cross markers represent the outliers, the horizontal red line in each box represents the median value, while the extent of the blue box is the interval of variation from the 25th to the 75th percentile.

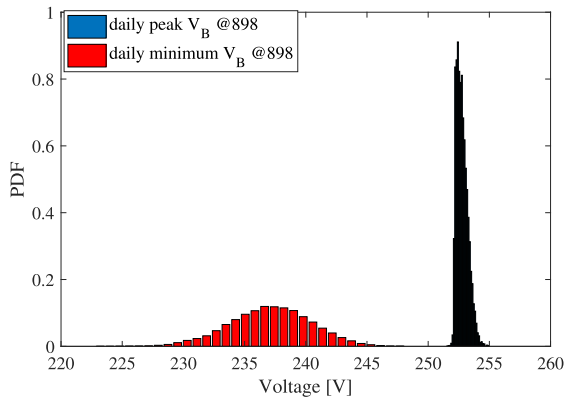


**FIGURE 6.** Distribution of the daily peak and minimum value for the Phase B at observable node 898.

uncertainty of the loads. With the proposed gPC+ST method, we calculate the detailed statistical distribution of the voltage minima and peak values for the same phase B at node 898. Fig. 6 shows, as an example, the distribution of the daily peak and minimum value for the Phase B at observable node 898.

It can be seen how, for the load distribution provided by the benchmark, Phase-B exhibits great variability of the minimum value, that ranges within the interval (232, 242) V with 90% probability. The peak value of Phase B, fluctuates within a narrower interval, i.e. about (252.5, 254) V, however its distribution is non Gaussian. This result is better seen in Fig. 7 where the statistical distributions of the Phase-B peak computed with the proposed gPC and with the reference MC method are reported and compared with the Gaussian distribution of equal mean value and variance.

Such a nonGaussian distribution of the node voltage is due to the nonlinearity of the PLF problem which is correctly reproduced by the gPC+ST model. It is worth noting how the MC method (implemented with a latin-hypercube sampling [18]) requires more than 5,000

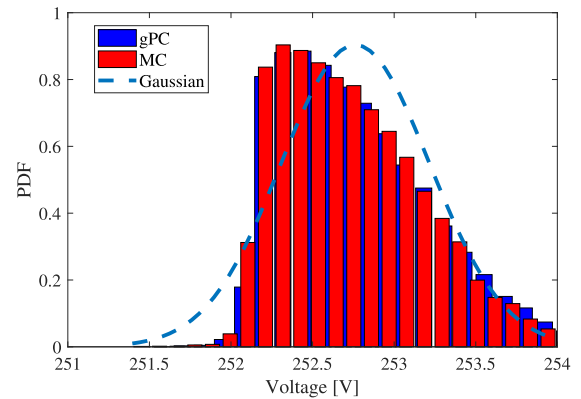


**FIGURE 7.** (Histogram) Detail of the distributions of the Phase-B daily peak value as computed with gPC and MC method (5,000 samples). (Blue Dashed Line) Gaussian distribution of equal mean value and variance.

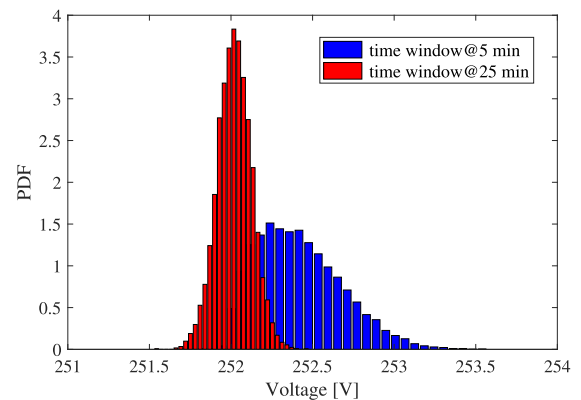


**FIGURE 8.** Distributions of  $V_W^{peak}$  of the Phase B at observable node 898 for different time durations.

samples

(i.e. deterministic load flow analyses) in order to obtain a sufficiently accurate estimation of the peak value distribution. With this setting, the peak value distributions provided by the proposed gPC and MC method are almost superimposed and the associated standard deviations, i.e.  $\sigma_{gPC} = 0.396$  V and  $\sigma_{MC} = 0.401$  V, match within a relative accuracy of 2%.

As a second example, Fig. 8 shows the distributions of the quantity  $V_W^{peak}$  defined in (15) (i.e., the maximum voltage level that is exceeded by the node voltage for a time duration  $W$ ) for time durations  $W = 5$  min and  $W = 20$  min. If a safe upper limit of  $V_L = 252.5$  V is assumed, by integrating the PDFs, we derive that there is a  $\approx 70\%$  probability that the Phase-B node voltage will exceed the upper limit for a time duration of five minutes. Such a probability reduces to zero for time durations of 25 minutes or longer. A further fundamental element to assess the quality of low voltage networks in the presence of single-phase loads is the voltage unbalance factor VUF defined in (17) along with the quantity  $VUF_W^{peak}$ , i.e. the VUF peak lasting for a sufficiently long time  $W$ . Fig. 9 shows the PDFs of  $VUF_W^{peak}$ , for three different

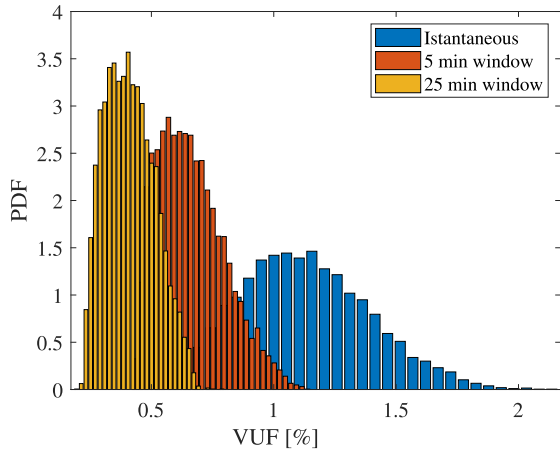


FIGURE 9. Distribution of voltage unbalance peak  $VUF_W^{peak}$  at 898 for three different time windows.

TABLE 1. Simulation times.

	2 Variables	3 variables	6 Variables
Number of Simulations	10	20	84
Total Time Elapsed [s]	113	241	1,455
Time per Simulation [s]	11	12	17

time windows. It is seen how the mean value of  $VUF_W^{peak}$  reduces as the observable time duration  $W$  is increased.

Finally, in Table 1, we report the simulation times of the proposed variability analysis (dominated by the deterministic load flow simulation with OpenDSS) for growing number of statistical parameters and fixed expansion order  $\beta = 3$ . For the case with  $l = 3$  parameters, one deterministic load flow analysis takes about 12 second and thus the variability analysis with the gPC method is completed in about 4 minutes. The same analysis with the same accuracy, performed with the accurate MC method (with 5,000 samples) takes more than sixteen hours.

**B. SCENARIO II: CHARGING POWER VARIATION FIXING THE LOADS**

In the second scenario we want to investigate what happens when electric vehicle charging stations are connected to a network that works with its instantaneous loads. In the hypothesis considered, let's imagine three charging points described by the base loads reported in the section III, one for each phase and installed at the nodes indicated in Fig. 3.

We consider only single-phase and slow recharging, as is considered in the TEINVEIN project [11], and suppose a smaller variation in power, as the loads have less uncertainty. This is due to the fact that the recharging of the vehicles of the considered fleet takes place in accordance with the scheduling established by the fleet manager and therefore with low variability.

According to the load model (2), we assume that the active powers  $P_{ev}(t)$  of all of the charging stations assigned to a given phase line, e.g. Phase A, are scaled by the same  $\xi$

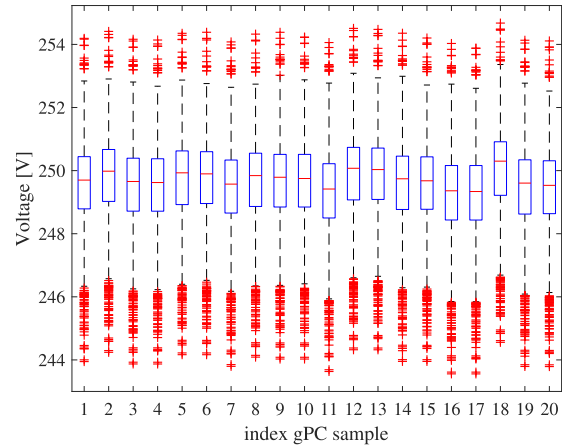


FIGURE 10. Scenario II. For each gPC sample the variation of the phase B voltage waveform is plotted. The red crosses represent the outliers, while the blue box is the interval of variation with the related median.

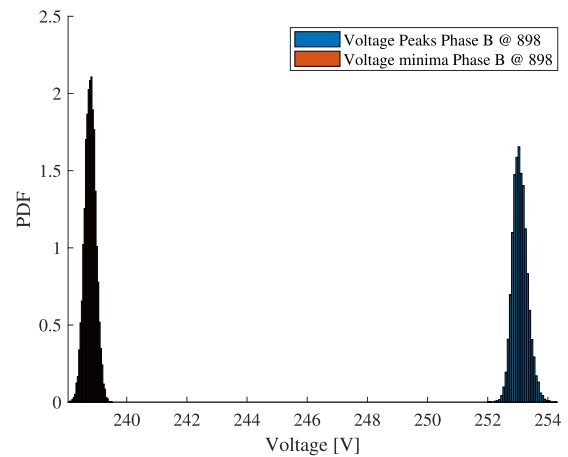


FIGURE 11. Distributions of daily voltage peak and minimum value of the Phase B at observable node 898 in the scenario II.

Gaussian statistical parameter, e.g.  $\xi_1$ , such as already done in the previous scenario. The degrees of variability are fixed equal and set to  $\sigma_{ev_1} = \sigma_{ev_2} = \sigma_{ev_3} = 0.08$  for all of the charging stations, that means a statistical variation smaller than 8%. Fig. 10 reports the boxplot of the B phase voltage waveform for each gPC sample. Fig. 11 shows, as in the previous scenario, the distribution of the daily peak and minimum value for the Phase B at observable node 898 This gives us a good idea about the variability of the peaks and minima voltage.

Particularly significant is the comparison between the peaks distributions (Fig. 12) in the two scenarios. This is due to the current values that induce higher voltages in this phase. It should be remembered that the test network is a network with all the lines described by means of auto and mutual inductance and the Phase B is the uncharged phase (The loads are in this example inserted in phase A and the EV in phase C). In this case there is no relevant voltage drop in this phase, nevertheless induced voltages due to the mutual coupling between the phases are present and strictly related to the current variation due to the EV charge

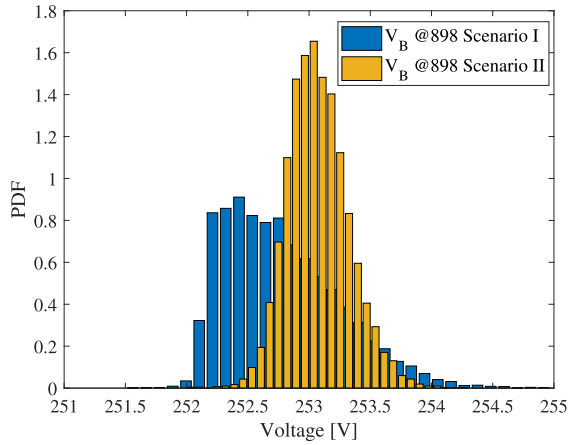


FIGURE 12. Comparison of the distributions of daily voltage peaks for the Phase B at observable node 898 in the two scenarios.

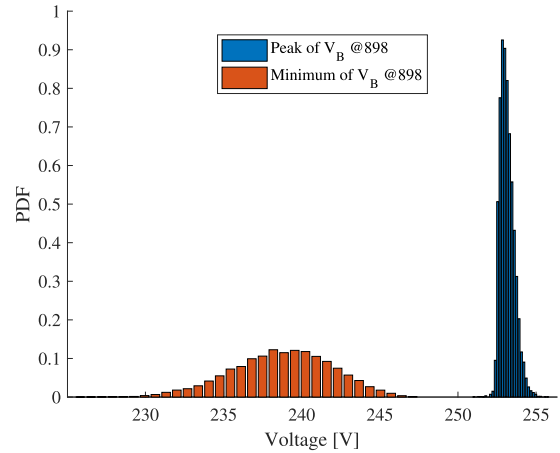


FIGURE 15. Distributions of daily voltage peak and minimum value of the Phase B at observable node 898 in the scenario III.

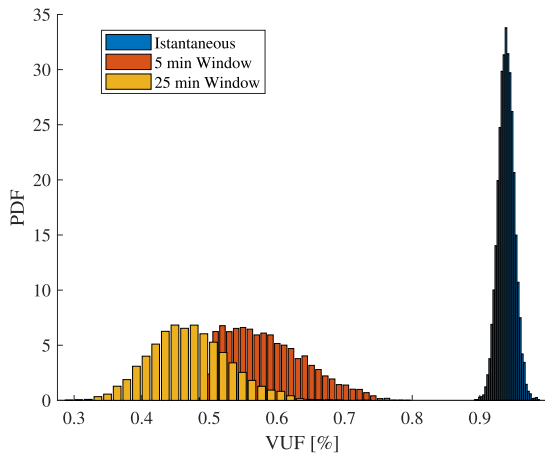


FIGURE 13. Distribution of voltage unbalance peak  $VUF_W^{peak}$  at observable node 898 for three different time windows in the case of electrical vehicle charging scenario.

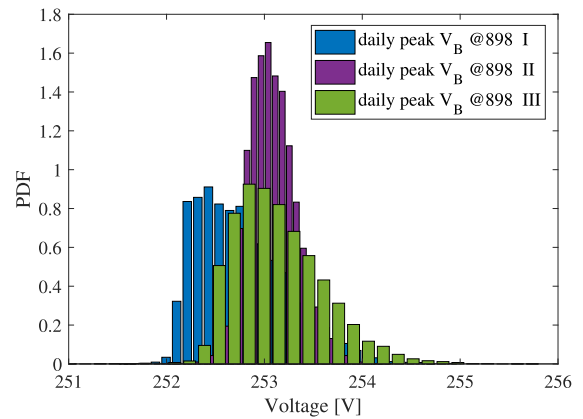


FIGURE 16. Comparison of Peaks distributions in the three different scenarios.

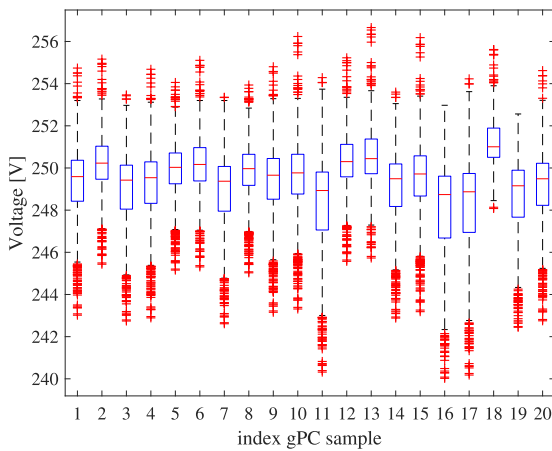


FIGURE 14. Scenario III. For each gPC sample the variation of the phase B voltage waveform is reported. The red cross represent the outliers, while the blue box is the interval of variation with the related median.

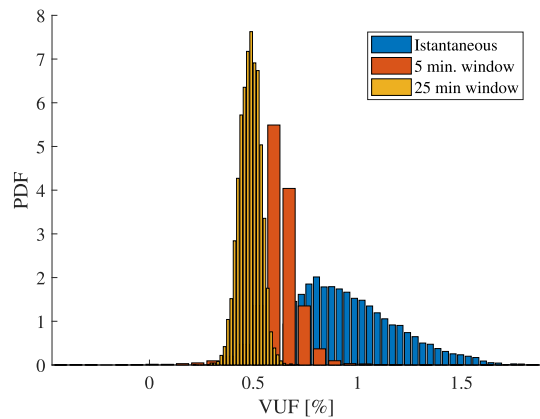


FIGURE 17. Distribution of voltage unbalance peak  $VUF_W^{peak}$  at node 898 for three different time windows in the scenario III.

Starting from the consideration that the trend of the powers absorbed by electric vehicles is more regular than those of residential loads, we can see that the instantaneous value of the voltage unbalance (Fig. 13) is lower in this scenario and is very far from the cases calculated on the window, a sign that the network has a higher quality of voltage in this case.

### C. SCENARIO III: CHARGING POWER AND LOADS VARIATIONS

In the last scenario both loads and vehicles are varied using the same parameters  $\xi$  and  $\sigma$  as in the two previous scenarios. It is assumed that the statistical variation is the same for each of the three phases, regardless of whether the load is

a charging station or a residential/commercial type. In this case the variability of the voltage in the considered node is very wide as shown in Fig. 14. Compared to the previous scenario, in this case the distribution of the minima changes and becomes wider, as well as the distribution of the maximums is very different from that obtained in scenario I as shown in Figs. 15 and 16.

The unbalance voltage in this scenario is more similar to that of scenario I, but the values involved are much lower. It may therefore be that the combined action of load variation and charge profile can lead to improvements in terms of voltage unbalances. This result depends a lot on the shape of the charging profile: from the data in our possession the charging profile is very constant and if connected on a normally uneven phase it contributes to keep the imbalance contained.

## VII. CONCLUSION

In this paper, we have presented an efficient computational technique for predicting the statistical distribution and variability interval of relevant observable variables in distribution networks due to loads uncertainty. The proposed technique is able to account for real data-based load profiles and can provide information which is relevant for assessing the quality of service. As an example, the method has been applied to a IEEE benchmark network by considering variability of the loads connected at the three phases and to real Electric Vehicle recharge data. We have shown how, in this example, the proposed gPC method is able to achieve a speed up factor in computation of about  $200\times$  compared to standard Monte Carlo simulation.

## REFERENCES

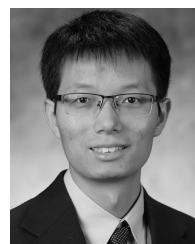
- [1] P. Samadi, H. Mohsenian-Rad, V. W. S. Wong, and R. Schober, "Tackling the load uncertainty challenges for energy consumption scheduling in smart grid," *IEEE Trans. Smart Grid*, vol. 4, no. 2, pp. 1007–1016, Feb. 2013.
- [2] P. Prempreaneerach, F. S. Hover, M. S. Triantafyllou, and G. E. Karniadakis, "Uncertainty quantification in simulations of power systems: Multi-element polynomial chaos methods," *Rel. Eng. Syst. Saf.*, vol. 95, no. 6, pp. 632–646, 2010.
- [3] J. M. Morales and J. Pérez-Ruiz, "Point estimate schemes to solve the probabilistic power flow," *IEEE Trans. Power Syst.*, vol. 22, no. 4, pp. 1594–1601, Dec. 2007.
- [4] K. Jhala, B. Natarajan, and A. Pahwa, "Probabilistic voltage sensitivity analysis (PVSA)—A novel approach to quantify impact of active consumers," *IEEE Trans. Power Syst.*, vol. 33, no. 3, pp. 2518–2527, May 2018.
- [5] Y. Wang, N. Zhang, Q. Chen, J. Yang, C. Kang, and J. Huang, "Dependent discrete convolution based probabilistic load flow for the active distribution system," *IEEE Trans. Sustain. Energy*, vol. 8, no. 3, pp. 1000–1009, Jul. 2017.
- [6] Z. Zhang, T. A. El-Moselhy, I. M. Elfadel, and L. Daniel, "Stochastic testing method for transistor-level uncertainty quantification based on generalized polynomial chaos," *IEEE Trans. Comput.-Aided Design Integr. Circuits Syst.*, vol. 32, no. 10, pp. 1533–1545, Oct. 2013.
- [7] Z. Zhang, T. A. El-Moselhy, P. Maffezzoni, I. M. Elfadel, and L. Daniel, "Efficient uncertainty quantification for the periodic steady state of forced and autonomous circuits," *IEEE Trans. Circuits Syst. II, Exp. Briefs*, vol. 60, no. 10, pp. 687–691, Oct. 2013.
- [8] G. Gruosso, P. Maffezzoni, Z. Zhang, and L. Daniel, "Probabilistic load flow methodology for distribution networks including loads uncertainty," *Int. J. Elect. Power Energy Syst.*, 106, pp. 392–400, Mar. 2019.
- [9] G. Gruosso, R. Netto, P. Maffezzoni, Z. Zhang, and L. Daniel, "Low voltage electrical distribution network analysis under load variation," in *Proc. IEEE Int. Conf. Ind. Technol.*, Feb. 2018, pp. 1248–1253.
- [10] (May 2015). *IEEE Distribution Test Feeders*. [Online]. Available: <http://ewh.ieee.org/soc/pes/dsacom/testfeeders/index.html>
- [11] L. Bascetta, G. Gruosso, and G. S. Gajani, "Analysis of electrical vehicle behavior from real world data: A V2I architecture," in *Proc. Int. Conf. Elect. Electron. Technol. Automot.*, Milan, Italy, 2018, pp. 1–4.
- [12] T. Wang and H.-D. Chiang, "On the global convergence of a class of homotopy methods for nonlinear circuits and systems," *IEEE Trans. Circuits Syst., II, Exp. Briefs*, vol. 61, no. 11, pp. 900–904, Nov. 2014.
- [13] D. K. Molzahn and I. A. Hiskens, "Convex relaxations of optimal power flow problems: An illustrative example," *IEEE Trans. Circuits Syst. I, Reg. Papers*, vol. 63, no. 5, pp. 650–660, May 2016.
- [14] D. Xiu and G. E. Karniadakis, "The Wiener–Askey polynomial chaos for stochastic differential equations," *SIAM J. Sci. Comput.*, vol. 24, no. 2, pp. 619–644, Feb. 2002.
- [15] A. Sandu, C. Sandu, and M. Ahmadian, "Modeling multibody systems with uncertainties. Part I: Theoretical and computational aspects," *Multibody Syst. Dyn.*, vol. 15, no. 9, pp. 373–395, Sep. 2006.
- [16] P. Pillay and M. Manyage, "Definitions of voltage unbalance," *IEEE Power Eng. Rev.*, vol. 21, no. 5, pp. 49–51, May 2001.
- [17] R. C. Dugan. (Mar. 2012). *Reference Guide The Open Distribution System Simulator (OpenDSS)*. [Online]. Available: <http://smartgrid.epri.com/SimulationTool.aspx>
- [18] M. Hajian, W. D. Rosehart, and H. Zareipour, "Probabilistic power flow by Monte Carlo simulation with latin supercube sampling," *IEEE Trans. Power Syst.*, vol. 28, no. 2, pp. 1150–1159, May 2013.



**GIAMBATTISTA GRUOSSO** (M'01–SM'12) was born in 1973. He received the M.S. and the Ph.D. degrees in electrical engineering from the Politecnico di Torino, Italy, in 1999 and 2003, respectively. From 2002 to 2011, he was an Assistant Professor with the Department of Electronics and Informatics, Politecnico di Milano, where he has been an Associate Professor, since 2011. His main research interests include electrical vehicles transportation electrification electrical power systems optimization, and simulation of electrical systems. He has authored more than 80 papers on journals and conferences on these topics. He is a Senior Member of the IEEE.



**GIANCARLO STORTI GAJANI** (M'12–SM'14) received the Dr. Ing. degree in electronic engineering and the Ph.D. degree in electronic systems from the Politecnico di Milano, in 1986 and 1991, respectively. Since 1992, he has been an Assistant Professor and has been an Associate Professor of circuit theory, since 2002. He has authored more than 90 papers in international journals and conferences. His research interests have been initially focused on the development of architectures for signal processing (in particular for audio and music applications) and neural networks. More recently, his research interests include non-linear circuits and non-linear dynamics. He is a Senior Member of the IEEE.



**ZHENG ZHANG** (M'15) received the B.Eng. degree from the Huazhong University of Science and Technology, in 2008, the M.Phil. degree from The University of Hong Kong, in 2010, and the Ph.D. degree in electrical engineering and computer science from the Massachusetts Institute of Technology (MIT), Cambridge, MA, USA, in 2015. He has been an Assistant Professor of electrical and computer engineering with the University of California at Santa Barbara, since 2017. His industrial experiences include Coventor Inc., Cambridge, MA, USA,

and Maxim-IC, Colorado Springs, CO, USA; academic visiting experiences include the University of California at San Diego, Brown University, and Politecnico di Milano, Milan, Italy; government laboratory experience includes the Argonne National Laboratory, Lemont, IL, USA. His research interests include uncertainty quantification and tensor computation with multi-domain applications, including CAD of nano-scale IC/MEMS/photonics, data analytics, machine learning, and autonomous systems. He received the Best Paper Award for the IEEE TRANSACTIONS ON COMPUTER-AIDED DESIGN OF INTEGRATED CIRCUITS AND SYSTEMS, in 2014, the Best Paper Award for the IEEE TRANSACTIONS ON COMPONENTS, PACKAGING AND MANUFACTURING TECHNOLOGY, in 2018, two Best Paper Awards (IEEE EPEPS 2018 and IEEE SPI 2016), and three additional Best Paper Nominations (CICC 2014, ICCAD 2011, and ASP-DAC 2011) at international conferences. His Ph.D. dissertation was recognized by the ACM SIGDA Outstanding Ph.D. Dissertation Award in Electronic Design Automation, in 2016, and by the Doctoral Dissertation Seminar Award (i.e., Best Thesis Award) from the Microsystems Technology Laboratory, MIT, in 2015. He was a recipient of the Li Ka-Shing Prize from the University of Hong Kong, in 2011.



**PAOLO MAFFEZZONI** (M'08–SM'15) received the Laurea degree (*summa cum laude*) in electrical engineering from the Politecnico di Milano, Italy, in 1991, and the Ph.D. degree in electronic instrumentation from Università degli Studi di Brescia, Italy, in 1996. He is currently a Full Professor of electrical engineering with the Politecnico di Milano. He has published about 140 research papers in international journals and conferences. His current research interests include modeling

and simulation of nonlinear circuits and systems, oscillatory devices, stochastic simulation, and unconventional computing with applications to analog and mixed-signal electronics and power systems. He served as an Associate Editor for the IEEE TRANSACTIONS ON COMPUTER-AIDED DESIGN OF INTEGRATED CIRCUITS AND SYSTEMS and the IEEE TRANSACTIONS ON CIRCUITS AND SYSTEMS I: REGULAR PAPERS.

...



**LUCA DANIEL** received the Ph.D. degree in electrical engineering from the University of California at Berkeley, in 2003. He is currently a Full Professor with the Electrical Engineering and Computer Science Department, Massachusetts Institute of Technology (MIT). Industry experiences include HP Research Labs, Palo Alto (1998), and Cadence Berkeley Labs (2001). His current research interests include integral equation solvers, uncertainty quantification and parameterized model order reduction, applied to RF circuits, silicon photonics, MEMs, magnetic resonance imaging scanners, and the human cardiovascular systems. He was a recipient of the 1999 IEEE TRANSACTIONS ON POWER ELECTRONICS Best Paper Award; the 2003 Best Ph.D. Thesis Awards from the Electrical Engineering Department and the Applied Math Department with UC Berkeley; the 2003 ACM Outstanding Ph.D. Dissertation Award in Electronic Design Automation; the 2009 IBM Corporation Faculty Award; the 2010 IEEE Early Career Award in Electronic Design Automation; the 2014 IEEE TRANSACTIONS ON COMPUTER-AIDED DESIGN Best Paper Award; and ten awards in conferences. He recently received the 2016 Teaching Award from the School of Engineering, MIT.